Earthquakes and Structures, Vol. 3, No. 3-4 (2012) 507-518
DOI: http://dx.doi.org/10.12989/eas.2012.3.3.507

Some properties of the Green's function of simplified elastodynamic problems

Francisco J. Sánchez-Sesma*[1], Alejandro Rodríguez-Castellanos[2], Juan J. Pérez-Gavilán[1], Humberto Marengo-Mogollón[3], Luis E. Pérez-Rocha[4] and Francisco Luzón[5]

[1]*Instituto de Ingeniería, Universidad Nacional Autónoma de México, Cd. Universitaria, Coyoacán 04510, México D F, Mexico*
[2]*Instituto Mexicano del Petróleo, Eje Central Lázaro Cárdenas 152, CP 07730, México D F, Mexico*
[3]*Coordinación de Proyectos Hidroeléctricos, Comisión Federal de Electricidad, Av. Río Mississippi 71, CP 06500, México D F, Mexico*
[4]*División de Sistemas Mecánicos, Instituto de Investigaciones Eléctricas, Reforma 113, Col. Palmira, CP 62490, Morelos, Mexico*
[5] *Depto. Física Aplicada, U de Almería, Cañada de San Urbano s/n, 04120-Almería, Spain*

(Received December 7, 2011, Revised March 7, 2012, Accepted April 10, 2012)

Abstract. It is now widely accepted that the resulting displacement field within elastic, inhomogeneous, anisotropic solids subjected to equipartitioned, uniform illumination from uncorrelated sources, has intensities that follow diffusion-like equations. Typically, coda waves are invoked to illustrate this concept. These waves arrive later as a consequence of multiple scattering and appear at "the tail" (*coda*, in Latin) of seismograms and are usually considered an example of diffuse field. It has been demonstrated that the average correlations of motions within a diffuse field, in frequency domain, is proportional to the imaginary part of Green's function tensor. If only one station is available, the average autocorrelation is equal to the average squared amplitudes or the average power spectrum and this gives the Green's function at the source itself. Several works address this point from theoretical and experimental point of view. However, a complete and explicit analytical description is lacking. In this work we study analytically some properties of the Green's function, specifically the imaginary part of Green's function for 2D antiplane problems. This choice is guided by the fact that these scalar problems have a closed analytical solution (Kausel 2006). We assume the diffusiveness of the field and explore its analytical consequences.

Keywords: diffuse fields; energy density; Green's function; correlations

1. Introduction

Coda waves, the long lasting vibrations from earthquakes are a clear evidence of multiple scattering within the Earth. They sample the medium around the recording station. For this reason coda waves are relevant in seismology and earthquake engineering. Various scattering formulations have been developed in order to explain the wave propagation in the heterogeneous earth (Sato and Fehler 1998). An equipartitioned diffuse field may exist in a given region if the net flux of energy

*Corresponding author, Ph.D., E-mail: sesma@unam.mx

is null. This condition is approximately met by coda waves as they continue ringing for a duration which is much longer than the source-station travel time. In fact, due to multiple scattering, coda waves arrive at a given site from different directions and sample the medium more or less uniformly around a recording station. These facts also apply to seismic noise.

There is growing interest in exploiting the information included in ambient seismic vibrations. These are used for the characterization of urban areas in seismic hazard studies (e.g. Pitilakis *et al.* 2011) and for the identification of dynamic properties in a variety of systems like bridges (e.g. Ali and Okabayashi 2011). If the illumination is uniform; that is to say, the sources of vibration are random and uncorrelated (multiple scattering due to complexity of systems contribute to achieve this) we can have realizations of diffuse fields. In that case, the available energy is equally distributed, in fixed average amounts, among all the possible states of the system. This is one way to formulate the equipartition principle. These ideas from thermodynamics have been introduced into room acoustics and elastic wave propagation by Weaver (1982).

The system's response to an impulsive unit load or Green's function can be retrieved from average cross correlations of recorded motions of a diffuse field (Campillo 2006, Sánchez-Sesma and Campillo 2006, Snieder *et al*. 2006, Wapenaar *et al.* 2007, Sánchez-Sesma *et al.* 2006). The pioneering studies of Aki (1957) and Aki and Chouet (1975) contributed to the understanding of coda waves and seismic noise.

Formal identities between the Green's function and correlations of the diffuse field for general inhomogeneous media have been established (Weaver and Lobkis 2004). In fact, the result for the homogeneous case (Sánchez-Sesma and Campillo 2006) also emerged for a homogeneous medium with a circular cylindrical elastic inclusion (Sánchez-Sesma *et al.* 2006, Pérez-Ruiz *et al.* 2008). This result was extended for elastic inhomogeneous media (Sánchez-Sesma *et al.* 2008) and has been used to explain numerically the coda of Green's functions (Sato 2010).

In this communication we consider some 2D scalar problems that have complete analytical solutions. This is not always the case and it is remarkable because considerable insight can be gained from these canonical cases. For a single receiver we compute the autocorrelation which is proportional to the energy density at a given point. Thus, we explore the consequences of assuming both source and receiver at the same point. In this case the imaginary part of the Green's function at the source itself is finite because the singularity is restricted to the real part. Moreover, the imaginary part of Green's function is proportional to the energy injected into the medium by the unit harmonic load (Sánchez-Sesma *et al.* 2008).

The direct knowledge of the Green's function may allow establishing the energy density of a diffuse seismic field. In seismology and engineering it is of interest having a theoretical interpretation of autocorrelations. In fact, it has been shown that nearby boundaries or heterogeneities induce fluctuations of energy densities in both space and frequency (Sánchez-Sesma *et al.* 2008).

2. Representation theorem of the correlation type

Consider an elastic, inhomogeneous, anisotropic domain V bounded by the surface Γ. Starting from the classical Betti-Rayleigh reciprocity identity, also known as the Somigliana's representation theorem (Sánchez-Sesma *et al.* 2008), it is possible to obtain a correlation type representation theorem

$$2i\mathrm{Im}[G_{mn}(\mathbf{x_A},\mathbf{x_B})] = -\int_\Gamma \{G_{mi}(\mathbf{x_A},\xi)T^*_{in}(\xi,\mathbf{x_B}) - G^*_{ni}(\mathbf{x_B},\xi)T_{im}(\xi,\mathbf{x_A})\}d\Gamma_\xi \tag{1}$$

where $G_{mn}(\mathbf{x}_A, \mathbf{x}_B)$ = displacement at $\mathbf{x}_A$ in direction m produced by a unit harmonic point force acting at $\mathbf{x}_B$ in direction n (this is the Green's function), the points $\mathbf{x_A}$ and $\mathbf{x_B}$ are located in V, $T_{im}(\mathbf{x}, \mathbf{x_A})$ = traction at point $\mathbf{x}$ in direction i, associated to the unit vector $n_i(\mathbf{x})$, produced by the unit harmonic point force in direction m acting at point $\mathbf{x_A}$ (this is the traction Green's function). In this identity, the imaginary part of the Green's tensor between points $\mathbf{x_A}$ and $\mathbf{x_B}$ is expressed in terms of boundary sources. The symbol * represents the complex conjugate, i is the imaginary unit and Im expresses the imaginary part. The dependence on angular frequency ω, of the Green's functions is understood and is omitted henceforth. For antiplane problems the subscripts for both displacements and tractions and for the associated Green's functions are restricted to be the value 2.

This representation theorem was presented before (Wapenaar 2004, van Manen *et al.* 2006) with a somewhat different notation. The equation is implicit in the treatment by Weaver and Lobkis (2004).

3. Retrieval of the Green's function from correlations

The field within V can be represented, as in Sánchez-Sesma and Campillo (1991), by the elastic radiation of force densities $\phi_i(\xi)$ acting along its boundary Γ

$$u_m(\mathbf{x}) = \int_\Gamma G_{mi}(\mathbf{x},\xi)\phi_i(\xi)d\Gamma_\xi \tag{2}$$

where $u_m(\mathbf{x})$ = displacement associated to the direction m at point $\mathbf{x}$. It is usual to define a diffuse field in terms of given force densities such that their average along Γ is null; here we represent the average with brackets, thus $\phi_i(\xi) = 0$, and assume that $\phi_i(\xi)$ and $\phi_j(\xi)$ are uncorrelated. As a consequence of these assumptions we have (see Wapenaar 2004)

$$\langle \phi_i(\xi)\phi^*_j(\zeta)\rangle = F^2\delta_{ij}\delta(\xi-\zeta) \tag{3}$$

where F^2 is the spectral density of the excitation and δ_{ij} is the Kronecker symbol ($\delta_{ij} = 1$ if $i = j$ or $\delta_{ij} = 0$ if $i \neq j$).

The average cross correlation of motion at points $\mathbf{x_A}$ and $\mathbf{x_B}$ is then given by

$$\langle u_m(\mathbf{x_A})u^*_n(\mathbf{x_B})\rangle = \int_\Gamma\int G_{mi}(\mathbf{x_A},\xi)G^*_{nj}(\mathbf{x_B},\zeta)\langle \phi_i(\xi)\phi^*_j(\zeta)\rangle d\Gamma_\xi d\Gamma_\zeta \tag{4}$$

Therefore

$$\langle u_m(\mathbf{x_A})u^*_n(\mathbf{x_B})\rangle = F^2\int_\Gamma G_{mi}(\mathbf{x_A},\xi)G^*_{ni}(\mathbf{x_B},\xi)d\Gamma_\xi \tag{5}$$

3.1 Far field approximation for Green's tensor

From the exact expressions for Green's tensors for 2D (see Sánchez-Sesma and Campillo 2006), their far field asymptotic representations, for both displacements and tractions, in a homogeneous, isotropic, elastic medium are given by

$$G_{mi}(\mathbf{x_A}, \xi) \approx f_1(qr_\mathbf{A}) n_m n_i + f_2(kr_\mathbf{A})(\delta_{mi} - n_m n_i) \quad \text{and} \tag{6}$$

$$T_{in}(\xi, \mathbf{x_B}) \approx i\omega\rho[\alpha f_1(qr_\mathbf{B}) n_i n_n + \beta f_2(kr_\mathbf{B})(\delta_{in} - n_i n_n)] \tag{7}$$

respectively. In these equations $\mathbf{r_A}$ and $\mathbf{r_B}$ are the distances between the point ξ, at the boundary Γ, and the points $\mathbf{x_A}$ and $\mathbf{x_B}$, respectively. As the distances are very large, we assumed the unit vector n_j at the surface Γ to be equal for both points. $q = \omega/\alpha$ and $k = \omega/\beta$, are the wavenumbers, ω = angular frequency, α and β are the P and S wavespeeds, respectively. These expressions have an interesting form: the product $f_1(qr_\mathbf{A})n_m n_i$ is a tensor that represents the longitudinal part of the motion while $f_2(kr_\mathbf{A})(\delta_{mi} - n_m n_i)$ accounts for the transverse part. In Eq. (7) the tractions at ξ are formed by the sum of the paraxial radiation boundary conditions for P and S waves, respectively. Paraxial means that it is locally assumed 1D wave propagation along the radiated field.

The radial functions f_1 and f_2 in 2D are cylindrical functions and are given by

$$f_1(qr_\mathbf{A}) = \frac{1}{4i\rho\alpha^2} H_0^{(2)}(qr_\mathrm{A}) \text{ and } f_2(kr_\mathbf{A}) = \frac{1}{4i\rho\beta^2} H_0^{(2)}(kr_\mathrm{A}) \tag{8}$$

here $H_0^{(2)}(\cdot)$ = Hankel's function of zero order and the second kind, ρ = mass density, and r_A = distance between ξ and $\mathbf{x_A}$.

The tractions at point ξ on Γ for a unit point load in the direction n_i applied at point $\mathbf{x_B}$ can be written using the paraxial boundary conditions for both longitudinal and transverse components as

$$T_{in}(\xi, \mathbf{x_B}) \approx -i\omega\rho(\alpha G_{jn}(\xi, \mathbf{x_B}) n_j n_i + \beta G_{jn}(\xi, \mathbf{x_B})(\delta_{ji} - n_j n_i)) = \tag{9}$$

$$-i\omega\rho(\alpha n_j n_i + \beta(\delta_{ji} - n_j n_i)) G_{nj}(\mathbf{x_B}, \xi)$$

Therefore, Eq. (1) can be written as

$$\mathrm{Im}[G_{mn}(\mathbf{x_A}, \mathbf{x_B})] = -\omega\rho \int_\Gamma (\alpha n_i n_j + \beta(\delta_{ij} - n_i n_j)) G_{mi}(\mathbf{x_A}, \xi) G_{nj}^*(\mathbf{x_B}, \xi) d\Gamma_\xi \tag{10}$$

The resulting Green's tensors, at the boundary, share the asymptotic properties of functions f_1 and f_2 as defined in Eqs. (6)-(8).

From Eqs. (5) and (10), taking into account Eqs. (6)-(8) it is possible to write

$$\langle u_i(\mathbf{x_A}) u_j^*(\mathbf{x_B}) \rangle = -4E_S k^{-2} \mathrm{Im}[G_{ij}(\mathbf{x_A}, \mathbf{x_B})] \tag{11}$$

for 2D. $E_s = \rho\omega^2 S^2$, which represents the average energy density and S^2 = average spectral density of the plane shear waves of the isotropic background. $k = \omega/\beta$ is the shear wavenumber associated to E_S. Eq. (11) is the analytical consequence of the representation theorem Eq. (1) and has been verified for the full space (Sánchez-Sesma and Campillo 2006) and an elastic inclusion embedded in an elastic space (Sánchez-Sesma *et al.* 2006).

4. Energy densities in 2D antiplane cases

The aim of this writing is to explore the consequences of the theory when source and receiver coincide. To this end, we assume that $\mathbf{x}_A = \mathbf{x}_B$ and consider some 2D(x, z) antiplane problems (Eq. (11) with $i = j = 2$) i.e., the propagation of shear waves polarized in the horizontal plane (*SH* waves). The forcing and the motion are restricted to be in the y direction denoted with the index 2 in the equations. For the elastic problem, the average energy density can be expressed as twice the average kinetic energy to account for the strain energy.

In what follows we compute the theoretical energy density at the surface of an elastic layer. To this end let us rewrite Eq. (11)

$$E(\mathbf{x_A}) = \rho\omega^2\langle u_2(\mathbf{x_A})u_2^*(\mathbf{x_A})\rangle = -4\mu E_S \mathrm{Im}[G_{22}(\mathbf{x_A}, \mathbf{x_A})] \tag{12}$$

While the first equality is clear because the energy density at $\mathbf{x_A}$ is proportional to the average of the squared spectral density, the last term is proportional to the work done by the harmonic unit line load acting at $\mathbf{x_A}$. For a homogeneous full space $\mathrm{Im}[G_{22}(\mathbf{x_A}, \mathbf{x_A})] \equiv -1/4\mu$, μ = shear modulus, and $E(\mathbf{x_A}) \equiv E_S$ showing the consistency of the formulation. In what follows, we compute the antiplane Green's functions at the source for a half-space with free surface and a layer with different boundary conditions in order to assess the expected normalized energy density at given locations.

4.1 2D half-space. Antiplane SH problem.

For a half-space, the Green's function can be obtained easily by superimposing the mirror image of the reflection, these boundary reflections take into account the waves generated by the condition imposed by the free-stress surface (see Kausel 2006)

$$G_{22}(\mathbf{x_A}, \mathbf{x_B}) = \frac{1}{4i\mu}\{H_0^{(2)}(kr) + H_0^{(2)}(kr')\} \tag{13}$$

where $H_0^{(2)}(\cdot)$ is the cylindrical Hankel's function of zero order and second kind. This function can be expressed as $H_0^{(2)}(\cdot) = J_0(\cdot) - iY_0(\cdot)$, where $J_0(\cdot)$ and $Y_0(\cdot)$ are the Bessel's functions of zero order of first and second kind. r is the distance between the source and the receiver and r' is the distance between the image source and receiver. If no attenuation is considered, the imaginary part of the Green's function is given by

$$\mathrm{Im}[G_{22}(\mathbf{x_A}, \mathbf{x_B})] = \frac{-1}{4\mu}(J_0(kr) + J_0(kr')) \tag{14}$$

At the source $r = 0$ and $r' = 2z$. According to Eq. (12) the energy density is proportional to the imaginary part of the Green's function at the source point. We have only *SH* waves, thus we define the reference energy $E_\infty = \rho\omega^2 S^2 = E_s$. Recalling that $J_0(0) = 1$, we can write

$$E(z, \omega) = E_\infty(1 + J_0(2kz)) \tag{15}$$

This expression gives the energy density as a function of both frequency and depth. At the surface the energy density is constant and twice the value of the infinite space. In Fig. 1 we depict the ratio $E(kz)/E_\infty$ against kz, a normalized depth because $k = 2\pi/\Lambda$ with Λ = wave-length of shear waves. In

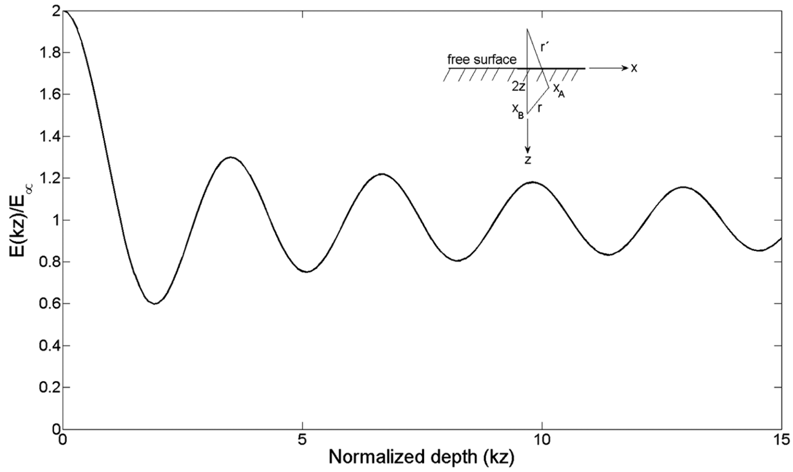

Fig. 1 Normalized energy density for a diffuse *SH* wave field in a 2D half-space

any event, the ratio depicted in Fig. 1 makes clear frequency dependent fluctuations with depth. The negative sign is included in the normalization. The reference energy E_∞ is the energy density in the 2D deep space. This is to say, where no energy amplification due to the presence of the free surface is observed.

4.2 2D layer. Antiplane SH waves

The energy variation of a diffuse elastic field at the surface of a 2D layer with thickness h is now studied. Consider first the problem that both layer boundaries are stress-free. We use again the images method, as in the half-space but now with infinite images to include all the reflections. The contribution to the imaginary part of Green function at source of the waves emitted is $\mathrm{Im}[1/(2i\mu)\,H_0^{(2)}(0)] = \mathrm{Re}[-(1/2\mu)H_0^{(2)}(0)] = -(1/2\mu)J_0(0) = -1/2\mu$, where Re[·] stands for the real part. This should be interpreted as the limit when the distance to observer tends to zero (see Snieder *et al.* 2009). The contributions of the reflections can be obtained by adding them all, each one with a free surface factor of two. Therefore, we can write

$$\mathrm{Im}[G_{22}(0,0)] = \mathrm{Re}\left[\frac{-1}{2\mu}\left(H_0^{(2)}(0)+2H_0^{(2)}(\omega\tau)+2H_0^{(2)}(2\omega\tau)+\cdots\right)\right] = \mathrm{Re}\left[\frac{-1}{2\mu}\sum_{n=0}^{\infty}\varepsilon_n H_0^{(2)}(n\omega\tau)\right] \quad (16)$$

where $\tau = 2h/\beta$ is the travel time for a single reflection. This expression was expressed using the Neumann factors ($\varepsilon_n = 1$ for $n = 0$ and $\varepsilon_n = 2$ for $n > 0$). Here n represents the natural numbers. This infinite sum is expressed with reciprocal square roots (Gradshteyn and Ryzhik 1994)

$$\mathrm{Im}[G_{22}(0,0)] = \frac{1}{2\mu\pi}\mathrm{Re}\left[\begin{array}{l} -\displaystyle\sum_{n=0}^{m}\frac{\varepsilon_n}{\sqrt{(f\tau)^2-n^2}} - \\ 2i\left(\pi/2\,Y_0(0) - C - \log\dfrac{f\tau}{2} + \displaystyle\sum_{n=1}^{m}\frac{1}{n} - \sum_{n=m+1}^{\infty}\left(\frac{1}{\sqrt{n^2-(f\tau)^2}} - \frac{1}{n}\right)\right)\end{array}\right] \quad (17)$$

where $f = \omega/2\pi$ is the frequency, m a natural number such that $\tau f - 1 < m < \tau f$, and C is the Euler constant. When no attenuation is taken into account, the second term inside the bracket is suppressed and the sum becomes finite. Damped media are treated with $\mu^* = \mu(1 + i/Q)$. The advantage of Eq. 17 is its faster convergence than Eq. 16 and the fact that the resonant frequencies n/τ of our free-free layer are explicit. Fig. 2 depicts the normalized energy density at the top of the layer for $\beta = 1$ and $h = 1$. The case of $Q = 50$ is also shown. Only the first five peaks are depicted. All the peaks of the undamped case are infinite. But, with the exception of the peak at the origin, which corresponds to the rigid body motion of the layer, all the other peaks are integrable.

Consider now that the layer is fixed at the depth h. The Green's function must thus be null at the bottom (this is the so called Dirichlet's boundary condition). Using the method of images, as previously, we can write

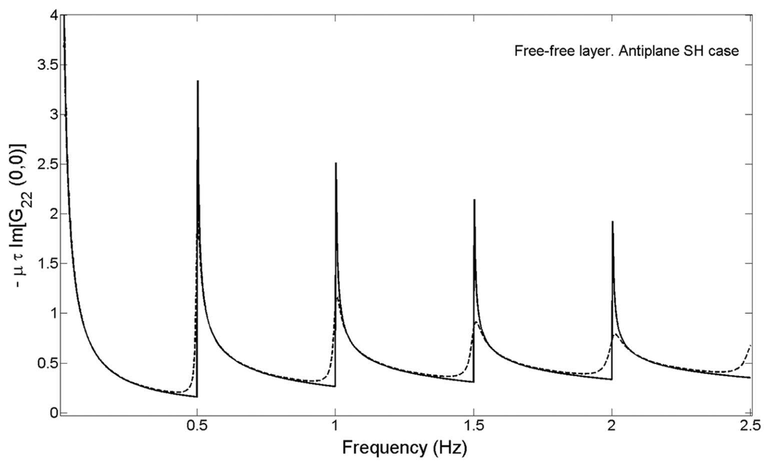

Fig. 2 Energy density at the origin, $-\mu\tau\,\mathrm{Im}[G_{22}(0,\,0)]$, against frequency in Hz. Results for a layer with stress-free boundary conditions without damping (solid line) and for $Q = 50$ (dashed line) are presented

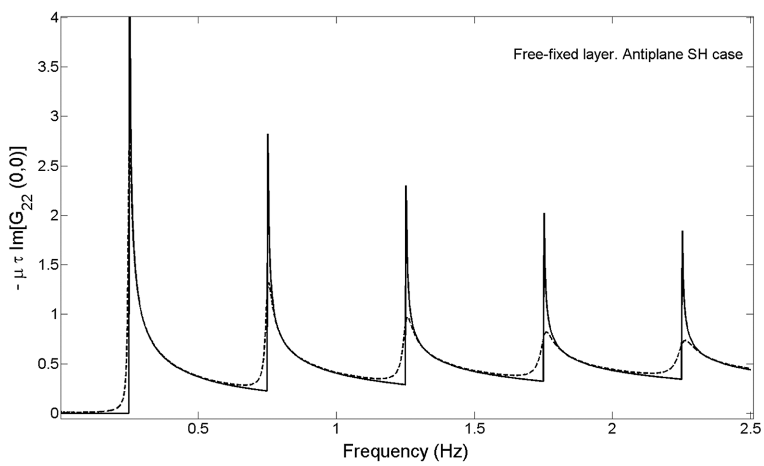

Fig. 3 Energy density at the origin, $-\mu\tau\,\mathrm{Im}[G_{22}(0,\,0)]$, against frequency in Hz. Results for a layer with stress-free and fixed boundary conditions without damping (solid line) and for $Q = 50$ (dashed line) are presented

$$\mathrm{Im}[G_{22}(0,0)] = \mathrm{Re}\left[\frac{-1}{2\mu}(H_0^{(2)}(0) - 2H_0^{(2)}(\omega\tau) + 2H_0^{(2)}(2\omega\tau) - 2H_0^{(2)}(3\omega\tau) + \cdots)\right] \tag{18a}$$

where again $\tau = 2h/\beta$ is the travel time for a single reflection. Because of the boundary condition at bottom there is a sign change for each reflection. The reflections are added and each appears with the free-stress surface factor of two. Using the Neumann factors ($\varepsilon_n = 1$ for $n = 0$ and $\varepsilon_n = 2$ for $n > 0$) it is possible to write

$$\mathrm{Im}[G_{22}(0,0)] = \mathrm{Re}\left[\frac{-1}{2\mu}\sum_{n=0}^{\infty}\varepsilon_n(-1)^n H_0^{(2)}(n\omega\tau)\right] \tag{18b}$$

The sum is transformed as before (see Gradshteyn and Ryzhik 1994)

$$\mathrm{Im}[G_{22}(0,0)] = \frac{1}{2\mu\pi}\mathrm{Re}\left[\begin{array}{l} -\sum_{n=1}^{m}\frac{2}{\sqrt{(f\tau)^2-(n-1/2)^2}} - \\ 2i\left(\pi/2Y_0(0) - C - \log\frac{f\tau}{2} + \sum_{n=1}^{m}\frac{1}{n} - \sum_{n=m+1}^{\infty}\left(\frac{1}{\sqrt{(n-1/2)^2-(f\tau)^2}} - \frac{1}{n}\right)\right)\end{array}\right] \tag{19}$$

where m verifies $\tau f - 1/2 < m < \tau f + 1/2$. These two conditions are depicted in Fig. 3, one without attenuation and the other with $Q = 50$. The first five peaks can be seen at the resonant frequencies $(n - 1/2)/\tau$ of the free-fixed layer. It is also clear that the frequency of the first peak is a cut-off frequency. For this we understand (putting aside the singularity of the real part) that lateral energy radiation is null for frequencies smaller than the cut-off one. In fact, for the rigid bottom all the modes are not propagating for these frequencies.

5. The time domain counterparts

Having the imaginary part of Green's function at the source we also have a description of the energy that is injected into the medium. For a homogeneous full space we have

$$\mathrm{Im}[G_{22}(\mathbf{x_A}, \mathbf{x_A}; \omega)] \equiv (-1/4\mu)\,\mathrm{sgn}\,\omega \tag{20}$$

where sgn $\omega = +1$ if $\omega > 0$ and sgn $\omega = -1$ if $\omega < 0$.

It is possible to show that

$$\frac{1}{2\pi}\int_{-\infty}^{\infty}\frac{-1}{4\mu}i\,\mathrm{sgn}\,\omega\exp(i\omega t)d\omega = \begin{cases}\frac{-1}{4\pi\mu}\times\frac{1}{t}, \text{for } t \neq 0\\ 0, \text{for } t = 0\end{cases} \tag{21}$$

which can be regarded as a particular case of

$$\frac{1}{2\pi}\int_{-\infty}^{\infty} i\frac{-1}{4\mu}J_0(\omega\tau)\,\mathrm{sgn}\,\omega\exp(i\omega t)d\omega = \begin{cases}\frac{1}{4\pi\mu}\times\frac{H(|t|-\tau)}{\sqrt{t^2-\tau^2}}\mathrm{sgn}\,t, \text{for } |t| > \tau\\ 0, \text{for } |t| < \tau\end{cases} \tag{22}$$

Eq. (21) exhibits the radiation into the medium composed of causal and anti-causal emission seismograms. On the other hand, for $\tau > 0$, Eq. (22) includes both causal and anti-causal seismograms, too.

From Eq. (16) and neglecting damping we have for the free-free layer.

$$\mathrm{Im}[G_{22}(0,0;\omega)] = \frac{-1}{2\mu}\sum_{n=0}^{\infty}\varepsilon_n J_0(\omega n\tau)\mathrm{sgn}\,\omega \tag{23}$$

here $\tau = 2h/\beta$. The time domain response, also called pseudo reflection seismogram, can be computed using Eq. (22) and is given by

$$\frac{1}{2\pi}\int_{-\infty}^{\infty} i\mathrm{Im}[G_{22}(0,0;\omega)]\exp(i\omega t)d\omega = \frac{1}{2\pi\mu}\sum_{n=0}^{\infty}\varepsilon_n\frac{H(|t|-n\tau)}{\sqrt{t^2-(n\tau)^2}}\mathrm{sgn}\,t \tag{24}$$

This result shows the emergence of reflections at times $t = n\tau = 2nh/\beta$ as it is shown in Fig. 4. There is other interesting fact that can be seen if we consider Eq. (17) without damping

$$\mathrm{Im}[G_{22}(0,0;\omega)] = \frac{-1}{2\mu\pi\tau}\sum_{m=0}^{\infty}\varepsilon_m\frac{H(|f|-m/\tau)}{\sqrt{f^2-(m/\tau)^2}}\mathrm{sgn}f \tag{25}$$

From Eqs. (24) and (25) we see a remarkable fact: the functional form of both the imaginary part of Green's function and the reflection seismograms is the same.

Now consider Eq. (18) and neglect damping. Then we have for our free-fixed layer.

$$\mathrm{Im}[G_{22}(0,0;\omega)] = \frac{-1}{2\mu}\sum_{m=0}^{\infty}\varepsilon_n(-1)^n J_0(\omega n\tau)\mathrm{sgn}\,\omega \tag{26}$$

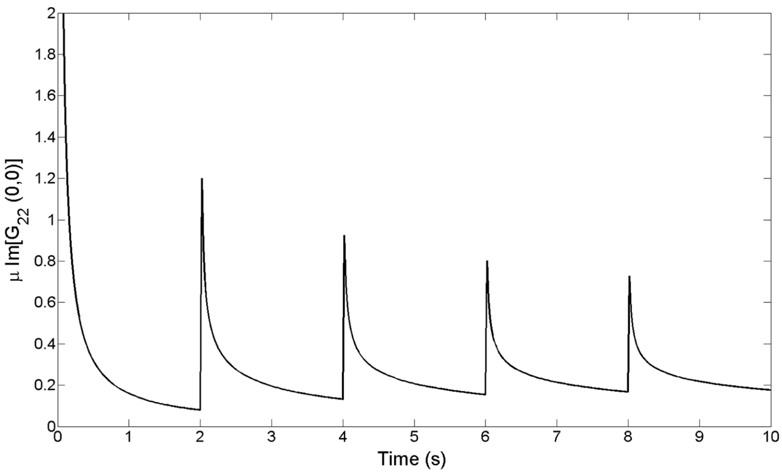

Fig. 4 Pseudo reflection seismogram for the free-free layer. Reflections at times $t = 2nh/\beta = n\tau$ ($\tau = 2s$) are observed

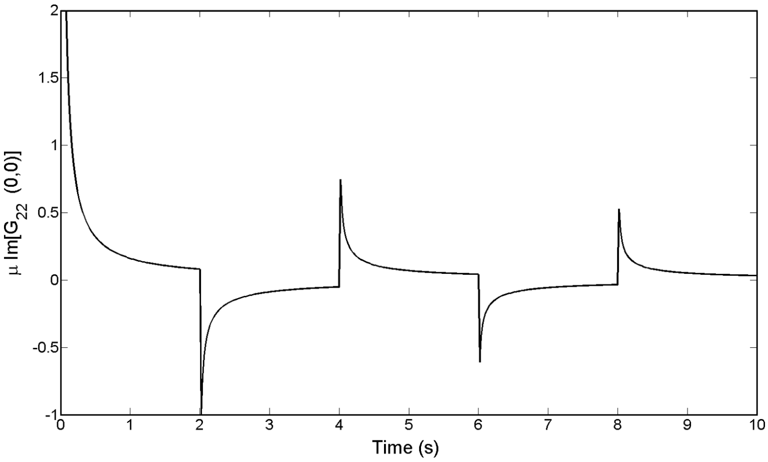

Fig. 5 Pseudo reflection seismogram for the free-fixed layer. Reflections at times $t = 2nh/\beta = n\tau$ ($\tau = 2s$) and changes in polarity are also seen

which can be expressed as

$$\mathrm{Im}[G_{22}(0,0;\omega)] = \frac{-1}{2\mu\pi\tau}\sum_{m=0}^{\infty}\frac{2H(|f|-(m+1/2)/\tau)}{\sqrt{f^2-(m+1/2)^2/\tau^2}}\mathrm{sgn}f \tag{27}$$

The pseudo-reflection seismogram, can be computed from Eqs. (26) and (22). It is given by

$$\frac{1}{2\pi}\int_{-\infty}^{\infty} i\mathrm{Im}[G_{22}(0,0;\omega)]\exp(i\omega t)d\omega = \frac{1}{2\pi\mu}\sum_{n=0}^{\infty}\varepsilon_n(-1)^n\frac{H(|t|-n\tau)}{\sqrt{t^2-(n\tau)^2}}\mathrm{sgn}t \tag{28}$$

This result shows both the emergence of reflections at times $t = n\tau = 2nh/\beta$ and the changes in polarity as it is depicted in Fig. 5 for positive times.

5. Discussion

In practical cases we do not have explicit expressions for the imaginary part of Green's function, instead we may have data. If the data displays stability and the average converges it is very likely that it converges to the imaginary part of the Green's function.

From Eq. (12) we propose to normalize the autocorrelations in such a way that the average is performed for windows in time, each with equal energy in the selected frequency band

$$\mathrm{Im}[G_{22}(\mathbf{x},\mathbf{x};\omega)] = \frac{-1}{4\mu}\left\langle\frac{\Omega|u_2(\mathbf{x};\omega)|^2}{\int_{\Omega}|u_2(\mathbf{x};\varpi)|^2 d\varpi}\right\rangle \tag{29}$$

Therefore, save for a multiplicative constant, the normalized autocorrelation in frequency domain may reveal resonant frequencies, amplification patterns and pseudo reflection seismograms that may give clues to uncover the medium geometry or properties.

6. Conclusions

In these work several properties of Green's functions are examined. Theoretical pseudo-reflection seismograms are obtained. We found functional forms of both the imaginary part of Green's function (in frequency) and the reflection seismograms (in time) that are remarkably similar.

The precise knowledge of Green's function in realistic cases cannot always be achieved. However, by means of measurements of ambient vibrations it is possible to generate reasonable realizations (say proxies) of the imaginary part of Green's functions with its properties (dispersion of surface waves, resonances and pseudo reflection seismograms).

At a given location in which ambient seismic vibrations exist, that can be regarded as realizations of a diffuse field, the average normalized autocorrelations, in frequency domain, is a measure of energy density, at least the relative frequency variations of such measurement are preserved.

From these results we can also point out that the diffuse field assumption may be helpful to generate spectral ratios in terms of the imaginary part of Green's function when both source and receiver coincide.

Acknowledgements

We dedicate this work to Professor José Manuel Roësset as a sincere homage for his fruitful carrier as engineer, scientist and teacher of many generations. Thanks are given to M. Campillo, V.J. Palencia, M. Perton, and R. Snieder for fruitful and enlightening discussions and to S. Anagnostopoulos and J.L. Tassoulas for their comments and suggestions. The suggestions of two anonymous reviewers helped to clarify the manuscript. We thank Guillermina Sánchez N. and her team of Unidad de Servicios de Información (USI) of Instituto de Ingeniería, UNAM, their help was crucial to locate useful references. Partial supports from DGAPA-UNAM, Project IN121709, Mexico; from Project CGL2010-16250, Spain; from FEDER, Spain; and from the Instituto Mexicano del Petróleo are greatly appreciated.

References

Aki, K. (1957), "Space and time spectra of stationary stochastic waves with special reference to microtremors", *Bull. Earthq. Res. Inst.*, **35**(3), 415-456.

Aki, K. and Chouet, B. (1975), "Origin of coda waves: Source, attenuation and scattering effects", *J. Geophys. Res.*, **80**(23), 3322-3342.

Ali, M.R. and Okabayashi, T. (2011), "System identification of highway bridges from ambient vibration using subspace stochastic realization theories", *Earthq. Struct.*, **2**(2), 189-206.

Campillo, M. (2006), "Phase and correlation in random seismic fields and the reconstruction of the Green function", *Pure Appl. Geophys.*, **163**(2-3), 475-502.

Gradshteyn, I.S. and Ryzhik, I.M. (1994), *Table of integrals, Series and products fifth edition*, Academic Press, London.

Kausel, E. (2006), *Fundamental solutions in elastodynamics, A Compendium*, Cambridge University Press, New York.

Pitilakis, K.D., Anastasiadis, A.I., Kakderi, K.G., Manakou, M.V., Manou, D.K., Alexoudi, M.N., Fotopoulou, S.D., Argyroudis, S.A. and Senetakis, K.G. (2011), "Development of comprehensive earthquake loss scenarios for a Greek and a Turkish city: Seismic hazard, geotechnical and lifeline aspects", *Earthq. Struct.*, **2**(3), 207-232.

Pérez-Ruiz, J.A., Luzón, F. and Sánchez-Sesma, F.J. (2008), "Retrieval of elastic Green's tensor near a cylindrical inhomogeneity from vector correlations", *Commun. Comput. Phys*., **3**(1), 250-270.

Sánchez-Sesma, F.J. and Campillo, M. (1991), "Diffraction of P, SV and Rayleigh waves by topographic features: A boundary integral formulation", *B. Seismol. Soc. Am*., **81**(6), 2234-2253.

Sánchez-Sesma, F.J. and Campillo, M. (2006), "Retrieval of the Green function from cross-correlation: The canonical elastic problem", *B. Seismol. Soc. Am*., **96**(3), 1182-1191.

Sánchez-Sesma, F.J., Pérez-Ruiz, J.A., Campillo, M. and Luzón, F. (2006), "The elastodynamic 2D Green function retrieval from cross-correlation: The canonical inclusion problem", *Geophys. Res. Lett*., **33**, L13305.

Sánchez-Sesma, F.J., Pérez-Ruiz, J.A., Luzón, F., Campillo, M. and Rodríguez-Castellanos, A. (2008), "Diffuse fields in dynamic elasticity", *Wave Motion*, **45**(5), 641-654.

Sato, H. (2010), "Retrieval of Green's function having coda waves from the cross-correlation function in a scattering medium illuminated by a randomly homogeneous distribution of noise sources on the basis of the first-order born approximation", *Geophys. J. Int*., **180**(2), 759-764.

Sato, H. and Fehler, M. (1998), *Wave propagation and scattering in the heterogeneous earth*, Springer-Verlag, New York.

Snieder, R., Wapenaar, K. and Slob, E. (2006), "Unified Green's function retrieval by cross correlation", *Phys. Rev. Lett*., **97**(4), 234-301.

Snieder, R., Sánchez-Sesma, F.J. and Wapenaar, K. (2009), "Field fluctuations, imaging with backscattered waves, a generalized energy theorem, and the optical theorem", *SIAM J. Imag. Sci*., **2**(2), 763-776.

Van Manen, D.J., Curtis, A. and Robertsson, J.O.A. (2006), "Interferometric modelling of wave propagation in inhomogeneous elastic media using time-reversal and reciprocity", *Geophysics*, **71**(4), S147-S160.

Wapenaar, K. (2004), "Retrieving the elastodynamic Green's function of an arbitrary inhomogeneous medium by cross correlation", *Phys. Rev. Lett*., **93**(25), 254301-1-4.

Wapenaar, K., Slob, E. and Snieder, R. (2007), Unified Green's function retrieval by cross correlation; connection with energy principles", *Phys. Rev. E.*, **75**(3), 036103(14).

Weaver, R.L. (1982), "On diffuse waves in solid media", *J. Acoust. Soc. Am*., **71**(6), 1608-1609.

Weaver, R.L. and Lobkis, O.I. (2004), "Diffuse fields in open systems and the emergence of the Green's function", *J. Acoust. Soc. Am*., **116**(5), 2731-2734.

SA